02

First principle studies of the optical spectra of $A_2Ca_2(CO_3)_3$ (A: Na, K) double carbonates under pressure

© Yu.N. Zhuravlev

Kemerovo State University,
650000 Kemerovo, Russia

e-mail: zhur@kemsu.ru

Received March 03, 2023
Revised September 27, 2023
Accepted September 28, 2023

Density functional theory methods with the B3LYP hybrid functional and the basis of a linear combination of localized atomic orbitals of the CRYSTAL17 program code were used to study the pressure dependences of the structural and optical properties of double carbonates $Na_2Ca_2(CO_3)_3$, $K_2Ca_2(CO_3)_3$. The parameters of the Birch-Murnaghan equation of state and linear compressibility moduli are determined. The coefficients of generation of the second harmonic, which characterize the nonlinear optical properties of these materials, are determined, and the frequencies and intensities of normal long-wavelength oscillations are calculated, from which the spectra of infrared absorption and Raman scattering of light are plotted by Gaussian expansion. The LO-TO splittings were estimated and the reflection spectra were plotted. It is shown that in the lattice region the spectra differ in the number and intensities of modes, while in the region of intramolecular vibrations of CO_3^{2-} atoms for both compounds they have a qualitatively similar form. For lattice and intramolecular vibrations, with increasing pressure, the rates of increase in wave numbers differ for each type of vibration. For oscillations of the $\nu 4$, $\nu 1$, $\nu 3$ types, the Grüneisen mode parameter is usually equal to 0.2−0.4. For out-of-plane deformations $\nu 2$, it is negative in $Na_2Ca_2(CO_3)_3$ and close to zero in $K_2Ca_2(CO_3)_3$.

Keywords: *ab initio*, carbonates, infrared absorption, Raman scattering, pressure, Grüneisen parameter.

DOI: 10.61011/EOS.2023.09.57341.4667-23

Introduction

K_2CO_3-$CaCO_3$ and Na_2CO_3-$CaCO_3$ systems feature prominently both in materials science (as sources of new nonlinear optical materials [1]) and in the Earth science (as subsystems that model phase relations in the fluxing component of mantle rocks responsible for the generation of deep-seated magmas [2,3]). Specifically, shortite $Na_2Ca_2(CO_3)_3$, which is transparent in the ultraviolet region, has been synthesized by the high-temperature solid-state method in [1] and exhibited a moderate second harmonic generation (SHG) response that was three times more intense than the reference one of KH_2PO_4 (KDP) [4]. In view of this, its electronic structure and optical properties have been analyzed in [1] via density functional theory (DFT) calculations. Shortite is also geologically significant, since its is found in melt inclusions hosted in deep mantle mineral associations and in carbonatite and kimberlite rocks [5,6].

Carbonates are useful in the context of understanding of the surface composition of planetary bodies and serve as important ecological markers. Certain data suggest that various types of carbonate minerals (e.g., shortite and nyerereite [7,8]) are present on the surface of Mars, Ceres, Enceladus, and Europa.

Rare mineral shortite has been found [9] among groundmass minerals in kimberlites in a number of localities across the globe. It may form as a result of several subsolidus reactions in multicomponent systems such as kimberlites in the course of breakdown of hexagonal phase $(Na,K)_2Ca(CO_3,SO_4)_2$ into $Na_2Ca_2(CO_3)_3$ and $K_3Na(SO_4)_2$. Under a pressure of ~ 1 at, shortite forms in reaction $Na_2Ca(CO_3)_2 \cdot 2H_2O + CaCO_3 = Na_2Ca_2(CO_3)_3 + 2H_2O$ above 328 ± 2 K [10]. $Na_2Ca_2(CO_3)_3$ has been identified in [11,12] as orthorhombic with space group *Amm*2 and a structure consisting of individual $NaCO_3$ and $Ca_2Na(CO_3)_2$ layers. Two sodium atoms (Na1 and Na2), one calcium atom (at disordered trigonal prismatic, sevenfold, and ninefold sites, respectively), and two different carbonate ions $C1O_3$ and $C2O_3$ are found in the lattice cell.

Experiments on phase relations in the K_2CO_3-$CaCO_3$-$MgCO_3$ system have been carried out in [13] at 3 GPa and 1023−1373 K, and $K_2Ca_2(CO_3)_3$ remaining stable within the entire temperature interval was obtained. The results of synthesis of double K-Ca carbonates under atmospheric pressure in closed graphite capsules have been reported in [14]. Mixtures of K_2CO_3 and $CaCO_3$ were used as starting materials, and compound $K_2Ca_2(CO_3)_3$ was synthesized in two ways: by solid-state synthesis at 873 K within 72 h and by cooling the melt from 1103 to 923 K within 30 min. The enthalpy of formation of double carbonate $K_2Ca_2(CO_3)_3$ has been determined by drop solution calorimetry in [15], and its thermal decomposition has been examined in [16]. Its hexagonal structure belongs to symmetry group $R3$ [17]. Two crystallographically different carbonate ions in it are located in columns around

the three-fold axis along which single cations Ca1 and K1 are positioned, and the remaining three Ca2 and K2 are located in general positions between the carbonate columns. Carbonate ions are inclined relative to the (001) plane and do not form a layered structure.

The study of $A_2Ca_2(CO_3)_3$ (A: Na, K) at high temperatures and pressures bears a relation to the behavior of alkali–carbonate systems in the upper mantle. Shortite has been examined in [18] by single-crystal synchrotron X-ray diffraction and Raman scattering spectroscopy under high pressures and after laser heating in order to gain an insight into the processes of carbon retention in the interior of the Earth. A spectroscopic study of natural shortite compressed up to 8 GPa in a diamond anvil cell has been carried out in [19]. It was found that as the pressure increases, almost all bands exhibit a positive shift with a rate of $1-4\,cm^{-1}$/GPa for lattice modes and 3.6 and 3.9 cm^{-1}/GPa for CO_3 stretching modes. X-ray data have been used in [20] to demonstrate that the symmetry of shortite remains stable under pressures up to 10 GPa. Diffraction data indicate that the volume decreases by 12% relative to its value under normal pressure. They also reveal that axis *c* is two times more compressible than axes *a* and *b*. This compression anisotropy is likely related to the orientation of relatively rigid carbonate groups: one third of them is oriented similar to plane *ab*.

Raman scattering (RS) and infrared (IR) absorption spectra are often used alongside with X-ray diffraction data to study the crystal structure of carbonate minerals. These spectra provide an opportunity to identify minerals, including those located on the surface of planetary bodies [7]. IR spectra of shortite within the range from 1660 to 1330 cm^{-1} are governed by vibrational mode $\nu 3$ (CO_3^{2-}); features within the 909–800 cm^{-1} range are attributed to modes $\nu 2$; and two bands at 731 and 696 cm^{-1} are produced by mode $\nu 4$. According to the data from [19], valence mode $\nu 1$ is split in RS spectra into two bands at $1071-1072$ and $1090-1091\,cm^{-1}$, which correspond to two separate carbonate regions present in the structure. Four bands in the $696-731\,cm^{-1}$ region belong to split deformation mode $\nu 4$. RS and IR spectra of shortite under normal conditions have been studied in [21], and the corresponding measurements at high temperatures and pressures (up to 623 K and 5 GPa) and under a pressure of 3 GPa have been performed in [22] and [2], respectively. Intense bands at 1078 and 1076 cm^{-1} and bands in the lattice region have been identified in [14] in RS spectra of $K_2Ca_2(CO_3)_3$. The authors have proposed to use these spectra as reference ones to identify microinclusions in mantle phenocrysts and xenoliths from kimberlites and other alkaline rocks.

Experimental data on the structural, thermodynamic, and dynamic properties of shortite are supplemented by the results of DFT calculations with local (LDA) and gradient (PBE) functionals that have been performed in [23]. No theoretical data on $K_2Ca_2(CO_3)_3$ are currently available, and no experiments into the influence of pressure on its structure have been carried out. In view of this, the present study was aimed at calculating the crystal structure and nonlinear optical and vibrational spectra of $Na_2Ca_2(CO_3)_3$ and $K_2Ca_2(CO_3)_3$ both under pressureless conditions and under pressures up to 7 GPa by ab initio DFT methods with a hybrid functional and a basis of localized orbitals. The obtained data should serve as a reference for identification and prediction of the properties of these carbonates in real-life environments.

Calculation method

Ab initio studies of the pressure dependences of structural and optical properties of carbonates were performed using the Hartree–Fock (HF) and density functional theory methods implemented in the CRYSTAL17 code [24]. The B3LYP hybrid functional, which is a combination of 20% HF exchange, the Becke exchange functional [25], and the LYP correlation functional [26], was used. Basis functions in the form of a linear combination of localized Gaussian atomic orbitals were chosen. All-electron basis sets for carbon, oxygen [27], sodium, and potassium [28] atoms were used. The thresholds controlling the accuracy of the Coulomb and exchange series were set to 8, 8, 8, 8, 16 [29]. The reciprocal space was sampled with a Monkhorst–Pack grid [30] with 302 *k*-points in the irreducible part of the Brillouin zone. The accuracy of the self-consistency procedure was no worse than 10^{-9} a.u. (1 a.u. is equal to 27.21 eV).

The frequencies of harmonic vibrations of lattice atoms were calculated using the procedure detailed in [31,32]. The authors of these studies have discussed the problem of numerical accuracy of the calculation of vibrational frequencies of crystalline compounds from the Hessian matrix:

$$W_{\alpha i,\beta j}(\Gamma) = \frac{H_{\alpha i,\beta j}}{\sqrt{M_\alpha M_\beta}},$$

where W is the second derivative of energy that is calculated numerically from analytical gradients, M_α and M_β are atomic masses, and Greek and Latin indices correspond to atoms and Cartesian coordinates, respectively. Frequencies ν_n at point G ($k = 0$, the center of the first Brillouin zone) were determined by diagonalizing matrix W, and oscillator strengths f_n were calculated for each *n*-mode with the use of the Born vector

$$Z_{n,i} = \Sigma_{\alpha,i} t_{n,\alpha j} Z^*_{\alpha,ij} \frac{1}{\sqrt{M_\alpha}}$$

($t_{n,\alpha j}$ is the element of eigenvectors of matrix W) as

$$f_{n,ij} = \frac{1}{4\pi\varepsilon_0} \frac{4\pi}{V} \frac{Z_{n,i} Z_{n,j}}{\nu_n^2}.$$

The IR absorption intensity was calculated using Born effective charge tensor $Z_{\alpha,ij)^*}$, which characterizes the electronic configuration change upon displacement of an atom and serves as its dynamic characteristic. The choice

of parameters governing the truncation of Coulomb and exchange series in HF, the quality of the grid used for numerical integration of the exchange-correlation potential in DFT, the convergence criteria, and the effects associated with the application of basis increasing in size were discussed. It was concluded that the error of these parameters does not exceed $2-4\,\mathrm{cm}^{-1}$ in relatively computationally inexpensive calculations. The results obtained with four different Hamiltonians (HF, DFT in its local (LDA) and nonlocal gradient corrected (PBE) approximations, and hybrid B3LYP), were also analyzed. It was demonstrated that B3LYP performs far better than LDA and PBE, which in turn provide better results than HF, as the mean absolute difference from experimental frequencies is 6, 18, 21, and $44\,\mathrm{cm}^{-1}$, respectively. The intensity of the Stokes line of the phonon mode is proportional to components α_{ii} of the polarizability tensor, and the relative intensities of peaks in RS spectra were calculated analytically using the procedure that is an extension of the analytical calculation of IR intensity [33].

The coupled perturbed Hartree–Fock (CPHF) method allows one to calculate linear and nonlinear optical properties of solid-state systems under periodic boundary conditions [34,35]. Correlation effects have been incorporated into the CPHF extension for the density functional theory (CPHF/KS) in B3LYP hybrid functionals in [36,37]. The dielectric susceptibility (polarizability) is the coefficient of linear relation between dielectric polarization P and electric field E:

$$P = \varepsilon_0(\chi^{(1)}E + \chi^{(2)}E^2 + \chi^{(3)}E^3 + \cdots,$$

where $\chi^{(2)}$ and $\chi^{(3)}$ are nonlinear second- and third-order susceptibilities that are calculated using the CPHF/KS procedure as in [38,39], where the tensors of static polarizability

$$\alpha_{tu} = \frac{\partial^2 E_{tot}}{\partial E_t \partial E_u}\Big|_0$$

and the first hyperpolarizability

$$\beta_{tuv} = \frac{\partial^3 E_{tot}}{\partial E_t \partial E_u \partial E_v}\Big|_0$$

are calculated as the corresponding field derivatives of total energy E_{tot}. The corresponding first and second susceptibilities are then determined in the following way:

$$\chi^{(1)}_{tu} = \alpha_{tu}\frac{4\pi}{V}, \quad \chi^{(2)}_{tuv} = \beta_{tuv}\frac{2\pi}{V}.$$

They have been calculated for crystalline urea in [39] with different basis sets and functionals: SVWN (local density approximation), PBE (generalized gradient approximation), PBE0 and B3LYP (hybrid), and Hartree–Fock. It turned out that the B3LYP hybrid functional in combination with a basis containing a containing a double set of polarization functions is remarkably successful in reproducing static linear and nonlinear optical properties, such as the dielectric constant, refraction and birefringence indices, and the first and second susceptibilities. The second-order susceptibility term leads to second-harmonic generation $d^{2\omega}_{ijk} = \chi^{(2)}_{ijk}/2$ (a. u.), and the third-order susceptibility term $\chi^{(3)}_{ijkl}$ is in charge of third-harmonic generation in induced RS [40].

The key quantity for IR spectra calculation is complex dielectric constant tensor $\varepsilon(\nu)$, which is calculated for each non-equivalent polarization direction based on the classical Drude–Lorentz model:

$$\varepsilon(\nu) = \varepsilon_{\infty,ij} + \Sigma_n \frac{f_{n,ii}\nu_n^2}{\nu_n^2 - \nu^2 - i\nu\gamma_n},$$

where ii denotes the polarization direction; $\varepsilon(\infty)$ is the static dielectric constant tensor at $\lambda \to \infty$; and ν_n, f_n , and γ_n are the frequency, the oscillator strength, and the decay coefficient for the nth vibrational mode, respectively. The maxima of the real part of $\varepsilon(\nu)$ correspond to transverse modes (TO), while the maxima of the imaginary part of $1/\varepsilon(\nu)$ correspond to the frequencies of longitudinal optical (LO) modes. Reflectance $R(\nu)$ [41] is calculated using the dielectric constant tensor.

The dependence of frequencies on pressure P (GPa) is characterized by Grüneisen mode parameter γ_i [42]:

$$\gamma_i = (B_0/\nu_i)(\partial\nu_i/\partial P),$$

where ν_i is the wave number of the ith vibrational mode (cm^{-1}), V is the corresponding lattice cell volume (Å^3), and B_0 (GPa) is the isothermal bulk compression modulus that is derived from the equation of state in the third-order Birch–Murnaghan form [43]:

$$P(V) = \frac{3B_0}{2}(x^{-7} - x^{-5})\Big(1 + \frac{3}{4}(B_1 - 4)(x^{-2} - 1)\Big),$$

$$x = (V/V_0)^{1/3},$$

and $B_1 = (\partial B/\partial P)_T$ is the first pressure derivative of the modulus at $x = 1$. Derivative $d\nu_i/dP$ of mode i with respect to pressure P is derived numerically from the quadratic interpolation of $\nu(P)$.

Crystal structure under pressure

A complete optimization of lattice constants and coordinates of atom positions was performed in order to determine the parameters of crystal structure of carbonates. Known literature data for $Na_2Ca_2(CO_3)_3$ (in what follows, it is referred to as Na-Ca) [11], $K_2Ca_2(CO_3)_3$ (K-Ca) were used as the initial ones [17]. Structural data determined in ab initio calculations are presented in Table 1. These theoretical data agree closely with the experimental ones: the mean-square deviations from [11] for lattice constants and all non-equivalent interatomic distances in Na-Ca do not exceed 1.58%; the corresponding deviations from parameters determined based on X-ray diffraction data are 1.14% [1] and 1.22% [5]. In K-Ca, the deviation from [17] is 1.74%.

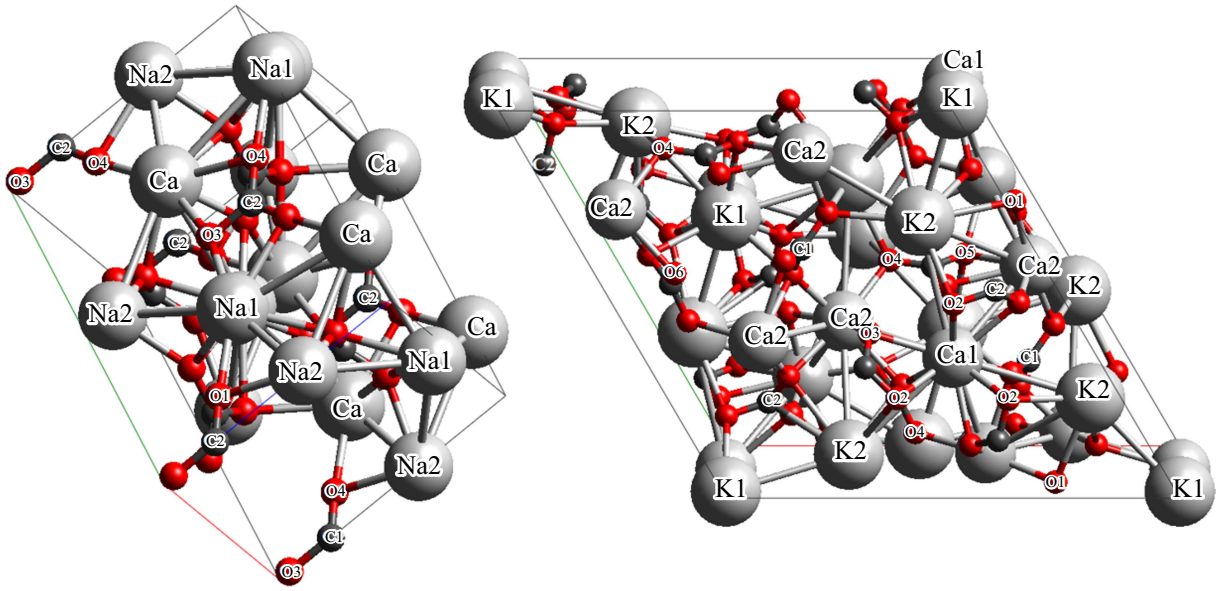

Figure 1. Crystal structure of $Na_2Ca_2(CO_3)_3$ (left) and $K_2Ca_2(CO_3)_3$ (right).

Table 1. Lattice constants a, b, and c (Å); volume V (Å^3) of a lattice cell; and mean distances between carbon C and oxygen O atoms (Å) calculated with B3LYP hybrid functionals and measured experimentally (Exp [Ref])

Method	a, Å	b, Å	c, Å	V, Å^3	C1-O(3)	C2-O(3)
$Na_2Ca_2(CO_3)_3$						
Exp [1]	4.9720(9)	11.068(3)	7.1271(14)	392.20(15)	1.2861	1.2978
Exp [5]	4.9571(3)	11.0514(6)	7.1242(4)	390.28(4)	1.2842	1.2985
B3LYP	4.9838	11.1076	7.2195	399.658	1.2869	1.3014
$K_2Ca_2(CO_3)_3$						
Exp [17]	13.010	13.010	8.615	1262.817	1.2746	1.2824
B3LYP	13.2148	13.2148	8.6837	1313.286	1.2892	1.2891

Table 2. Parameters V_0, B_0, and B_1 of the third-order Birch–Murnaghan equation of state and linear compression moduli B_a, B_b, and B_c along axes a, b, and c and for C-O bond lengths (all in GPa)

Crystal	V_0, Å^3	B_0, GPa	B_1	B_a	B_b	B_c	$B_{C1\text{-}3O}$	$B_{C2\text{-}3O}$
$Na_2Ca_2(CO_3)_3$	399.55	64.02	4.08	274.0	235.5	133.4	1226	1186
$K_2Ca_2(CO_3)_3$	1312.98	48.94	4.38	115.5	115.5	140.0	1146	1349

The crystal structures of Na-Ca and K-Ca with non-equivalent atoms indicated are shown in Fig. 1. The length of C1-O1 and C1-2O2 bonds in two $C1O_3$carbonate ions in the Na-Ca structure is 1.2776 and 1.2916 Å, respectively. The other $C2O_3$ ion has 1.2778 Å (C2-O4) and 1.3132 Å (C2-2O3). Each sodium atom Na1 is surrounded by eight oxygen atoms: two O1 (2.4844 Å), four O2 (2.5244 Å), and two O3 (2.6511 Å). Thus, the mean distance in the $Na1O_8$ polyhedron is 2.5461 Å (2.5293 Å in [5]). The other non-equivalent Na2 atom has six oxygen atoms (4O2 (2.3144 Å), 2O4 (2.4257 Å)) in the nearest-neighbor environment with the mean distance in $Na2O_6$ being 2.3515 Å (2.3397 Å in [5]). Each calcium atom is surrounded by nine oxygen atoms with the shortest Ca-O3 distance being 2.4256 Å and a mean Ca-O3 distance of 2.5299 Å (2.5061 Å in [5]). The chemical bond between cation and anion ions is markedly ionic, and the calculated Mulliken charges of sodium and calcium are $+0.94\,|e|$ (e is the electron charge) and

$+1.72\,|e|$; the corresponding charges of anions are -1.776 and $-1.782\,|e|$. The bond within CO_3^{2-} carbonate ions is covalent, which is evidenced by the electron charge present at the C-O bond line. Its overlap populations are 0.375 and 0.366 *e*.

Potassium atom K1 in the K-Ca structure is surrounded by six oxygen atoms (3O5, 3O2) at a mean distance of 2.7556 Å. Each of the three other equivalent atoms (K2) is surrounded by six oxygen atoms (2O4, 2O2, O6, O1) at a mean distance of 2.8072 Å. Calcium atoms also have two non-equivalent positions in this compound: Ca1 with nine surrounding oxygen atoms (3O6, 3O2, 3O3) with a mean distance of 2.5122 Å and three Ca2, each of them surrounded by seven oxygen atoms at 2.4582 Å. Six carbonate groups are present: three $C1O_3$ (O4, O5, O6) with a mean C1-O distance of 1.2892 Å and three $C2O_3$ (O_1, O_2, O_3) with a distance of 1.2891 Å. The corresponding charges are -1.753 and $-1.749\,|e|$—.

Uniform compression within the 0−7 GPa range was performed in order to examine the influence of pressure P on the structure. The structure was optimized at each pressure level with lattice cell volume V kept constant. The obtained $V(P)$ dependences were used to determine the parameters of the third-order Birch–Murnaghan equation of state, while the dependences of lattice constants $a(P)$, $b(P)$, and $c(P)$ and interatomic metal–oxygen $R_{\text{M-O}}(P)$ and carbon–oxygen $R_{\text{C-O}}(P)$ distances were used to find linear compression moduli $B_i = -x\partial P/\partial x$ (x: $a, b, c, R_{\text{M-O}}, R_{\text{C-O}}$). The parameters of the equation of state and linear compressibility moduli obtained this way are listed in Table 2.

The calculated and experimental [5] V_0 and B_0 values agree fairly closely. As the pressure rises, the lattice constants and interatomic distances decrease almost linearly in such a way that moduli $B_a(B_b)$ in carbonate Na-Ca are nearly two times greater than B_c. In contrast, $B_c > B_a$ in K-Ca, indicating that the compressibility along axis c is lower than the one along a. This anisotropy of compressibility along axes translates into different compressibilities of bonds. In double carbonate Na-Ca, the distances in $Na1O_8$ polyhedra decrease at a rate of -0.015 Å/GPa, while the corresponding rate is somewhat lower in $Na2O_6$ (-0.014 Å/GPa) and even less significant in CaO_9 (-0.013 Å/GPa). It follows from Table 2 that bonds C-O are virtually incompressible. The crystallographic nonequivalence of atoms also manifests itself under pressure. For example, the length of the shortest Na1-2O1 bond decreases at a rate of -0.025 Å/GPa (99.7 GPa), while the rate of reduction of the Na1-4O2 bond length is just -0.009 Å/GPa (280.5 GPa). This is attributable to the fact that the modulus for the C1-2O2 and C1-O1 bond lengths in carbonate ion $C1O_3$ is 1047 and 1875 GPa, respectively. In contrast, the length of the shortest Ca-O3 bond in CaO_9 polyhedra decreases at a lower rate (193.7 GPa) than the length of Ca-O4 (146.3 GPa), since the moduli for C2-O3 and C2-2O4 are 885.3 and 1436.8 GPa, respectively. These features should manifest themselves in vibrational spectra.

The compressibility of carbonate K-Ca is higher than the one of Na-Ca, since the potassium cation has a greater ionic radius than sodium. This is true both for the crystal in general and for its polyhedra. The bond compressibility moduli for $K1O_6$ and $K2O_6$ are 129.4 and 100.3 GPa. The same is true for calcium: $Ca1O_9$ — 166.0 GPa, $Ca2O_7$ — 212.1 GPa. The shortest C1-O4 bond and the longest C2-O1 bond have the highest compressibility in carbonate groups (869 and 774.6 GPa, respectively). Thus, the distances in polyhedra between cations with a greater ionic radius (Ca→K→Na) and oxygen atoms decrease at the highest rates under pressure in double carbonates, while the distances in carbonate ions remain almost unchanged.

Nonlinear optical properties

Ultraviolet (UV, wavelength $\lambda < 400$ nm) and deep ultraviolet (DUV, wavelength $\lambda < 200$ nm) lasers have a very high energy of individual photons, which makes them widely applicable in semiconductor photolithography, laser microprocessing, photochemical synthesis, medical and scientific device industry, and optoelectronic devices. However, it is not always possible to extract the wavelengths needed for these applications from a laser source itself. Therefore, second-harmonic generation (SHG) of nonlinear optical (NLO) materials is an important alternative way to produce the required wavelengths [44]. The design of new DUV and UV NLO materials with fine SHG characteristics and a short phase-matching cutoff wavelength is regarded at present as an important and challenging task [45].

Current and prospective NLO materials designed for practical applications should satisfy the following requirements with regard to their crystal structure: (i) have noncentrosymmetric (NCS) space groups of symmetry; (ii) contain anions in π-delocalized systems; and (iii) contain cations of transition metals sensitive to second-order Jahn–Teller distortions, stereochemically active cations with unshared electron pairs, or cations of transition metals with filled d^{10} shells and polar displacements [44]. As for their optical properties, the requirements are as follows [46]: (i) a short absorption edge or large energy bandgap (E_g); (ii) large SHG coefficients (d_{ij}), which should be greater than those of a standard sample, such as KH_2PO_4 (KDP, $d_{36} \approx 0.39$ pm/V); and (iii) moderate birefringence ($\Delta n = 0.07 - 0.1$), since it helps harmonic and fundamental radiation propagate at the same speed, facilitating phase-matching.

The studied crystals satisfy the above conditions. Their symmetry groups are NCS, and they belong to a wide class of carbonate NLO materials [46,47] with group CO_3^{2-} being a fine microstructural unit, since it features a planar triangular structure with π-conjugate molecular orbitals that produce a substantial second-order susceptibility. The bandgap of Na-Ca and K-Ca is 7.52 and 7.37 eV. The second-order susceptibility in Na-Ca calculated using the CPHF/KS method has nonzero components $\chi^{(2)}_{xxz} = 0.867$,

$\chi^{(2)}_{yyz} = 0.267$, and $\chi^{(2)}_{zzz} = -1.068$ a. u. This allows one to define the SHG coefficients in the Voigt notation in common units of measure: $d^{2\omega}_{15} = 0.845$ pm/V, $d^{2\omega}_{24} = 0.276$ pm/V, and $d^{2\omega}_{33} = -1.038$ pm/V. Birefringence index Δn is 0.0299, which is below the optimum value. The values of the corresponding macroscopic SHF coefficients have been derived in [48] with the use of the CNDO program from a geometric superposition of second-order susceptibilities of anion groups: 0.938, 0.088, −0.549 pm/V.

Since the symmetry of K-Ca is lower than the one of Na-Ca, a large number of components of the second-order susceptibility tensor are nonzero. Thus, the SHG coefficients here are $d^{2\omega}_{11} = -0.209$ pm/V, $d^{2\omega}_{16} = 0.724$ pm/V, $d^{2\omega}_{15} = -0.086$ pm/V, and $d^{2\omega}_{33} = 0.246$ pm/V. The birefringence index (0.0135) is even lower than in Na-Ca. Taken together with low SHG coefficients, this suggests that carbonate K-Ca should not be regarded as a promising NLO material.

Pressure affects the NLO properties of materials. As the pressure rises to 2 GPa, the SHG coefficients in carbonate Na-Ca decrease in absolute value at rates $\partial d^{2\omega}_{i\alpha}/\partial P$, which are equal to −0.01, −0.006, and 0.830 pm/(V·GPa) for $d^{2\omega}_{15}$, $d^{2\omega}_{24}$, and $d^{2\omega}_{33}$, respectively. Their mean value decreases from 0.455 to 0.442 pm/V. In contrast, the birefringence index increases to 0.0311. Index Δn does also increase to 0.014 in carbonate K-Ca. In this crystal, the SHG coefficients increase (in the order indicated above) to −0.158, 0.736 and −0.119, 0.297 pm/V, yielding a mean value of 0.205. This implies that pressure may be used to adjust the NLO properties of materials.

One should bear in mind that measurements of SHG coefficients are performed using the Maker interference method or the phase matching method, while the Kurtz–Perry technique [49] is used in experiments with powders. Individual $d^{2\omega}_{i\alpha}$ elements are often hard to measure in practice, since they get mixed. In addition, the coefficients have different signs in different measurement sets. This is the reason why complex studies combining measurements with ab initio calculations are needed.

Vibrational spectra

A lattice cell of orthorhombic carbonate Na-Ca contains 16 atoms; therefore, a total of 48 vibrational modes (three acoustical and 45 optical) should be present. The corresponding expansion of the full vibrational representation in irreducible ones takes the form

$$\Gamma_{vib} = 14A_1(\text{IR, RS}) + 7A_2(\text{RS}) + 14B_1(\text{IR, RS}) + \\ + 10B_2(\text{IR, RS}).$$

IR denotes the activity in infrared spectra with polarization A_1 — $\mathbf{E}\|\mathbf{z}$, B_1 — $\mathbf{E}\|\mathbf{y}$, B_2 — $\mathbf{E}\|\mathbf{x}$, while RS is the activity of Raman scattering with nonzero tensor components $A_1(\alpha_{xx}, \alpha_{yy}, \alpha_{zz})$, $A_2(\alpha_{xy})$, $B_1(\alpha_{yz})$, $B_2(\alpha_{xz})$. The expansion of the vibrational representation in irreducible ones for hexagonal carbonate K-Ca with 32 atoms is written as

$$\Gamma_{vib} = 31A(\text{IR, RS}) + 31E(\text{IR, RS}).$$

The polarization is fairly obvious here: A — $\mathbf{E}\|\mathbf{z}$, E — $\mathbf{E}\|xy$, $A(\alpha_{xx} = \alpha_{yy}, \alpha_{zz})$, $E(\alpha_{xx} = \alpha_{yy}, \alpha_{xy}, \alpha_{xz} = \alpha_{yz})$.

Carbonate spectra are distinct in that their vibrational modes are divided into lattice (0−400 cm^{-1}) and intramolecular ones of four types: deformations in the anion plane ($\nu 4$, 650−720 cm^{-1}), out-of-plane deformations ($\nu 2$, 840−910 cm^{-1}), symmetric stretching ($\nu 1$, 1000−1100 cm^{-1}), and asymmetric stretching vibrations ($\nu 3$, 1350−1600 cm^{-1}) [50,51]. A total of 18 intramolecular vibrations distributed over symmetries as $7A_1 + 2A_2 + 6B_1 + 3B_2$ should be observed in Na-Ca; vibrations $\nu 4$, $\nu 3$ in IR have symmetry $2A_1 + 2B_1 + B_2$, while $\nu 2$ and ν_1 have $A_1 + B_1 + B_2$. In RS spectra, a vibration of the A_2 symmetry is added for $\nu 4$, $\nu 3$.

Figure 2 presents the IR absorption and RS spectra for carbonate Na-Ca obtained by Gaussian broadening of normal long-wave vibrations at point G. The wave numbers of normal long-wave vibrations are listed in Table 3. For clarity, the spectra are divided into three wave number regions with similar vibration intensities. The intensity of mode $\nu 3$ of symmetry B_1 with a wave number of 1495.7 cm^{-1} and a value of 2827 km/mol was taken as 100% in IR. The mode of symmetry B_2 with a wave number of 1432.3 cm^{-1} has a similar intensity value (2688 km/mol). Vibration polarizations are color-coded. Green, purple, blue, and red colors correspond to symmetries A_1, A_2, B_1, and B_2, respectively. The maximum (100%) intensity in the RS spectrum has the mode of symmetry A_1 with a wave number of 1095.4 cm^{-1}. The intensity of the mode of the same symmetry and a wave number of 1078.5 cm^{-1} is lower (39%).

Three vibrations of symmetries A_1, B_2, and B_1 with wave numbers of 193.8 cm^{-1}, 225.7 cm^{-1} , and 284.8 cm^{-1} are dominant in the IR lattice region for carbonate Na-Ca. The relative amplitudes of displacements of non-equivalent atoms in a lattice cell, which are shown in Fig. 3, were used to determine the nature of individual vibrational modes. Specifically, z-displacements of atoms Na1, Na2, C2, O3 and yz displacements of the other atoms contribute to the vibration of symmetry A_1; notably, Na and $C2O_3$ move toward each other. The contributions of sodium atoms, Ca, and $C1O_3$ to the overall vibration amplitude are 25, 19, and 50%, respectively. In the case of symmetry B_2, sodium, calcium, and CO_3 vibrate along axis x in counter directions. The contributions of their amplitudes for Na2, Ca, $C1O_3$, and $C2O_3$ are 8, 13, 63, and 15%, respectively. The pattern of vibrations for symmetry B_1 is similar to A_1, but the direction changes to axis y. The contribution of Na2 here increases to 23%, calcium provides 18%, $C1O_3$ gives 10%, and $C2O_3$ is dominant with 49%. Two intense (10 and 7%) modes with symmetries B_2, A_1 and wave numbers of 263.3 and 274.8 cm^{-1} may be distinguished in the RS

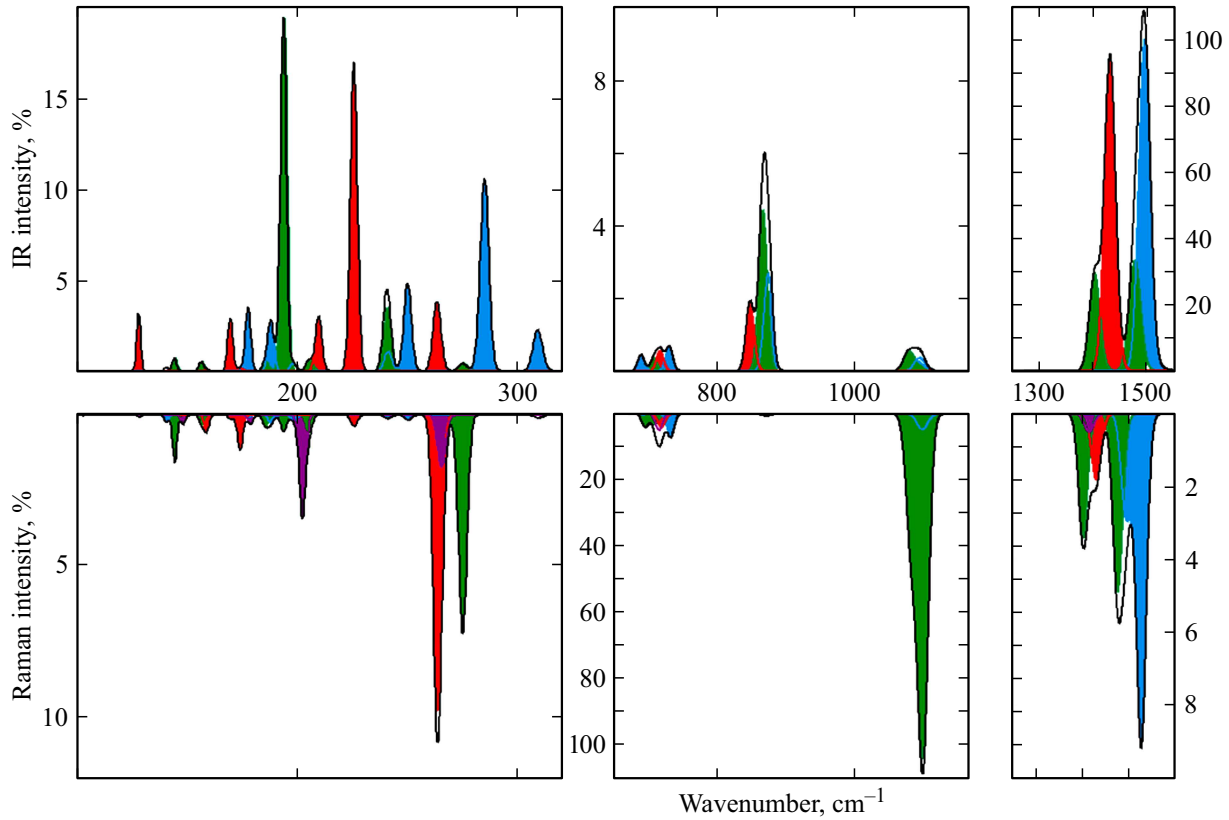

Figure 2. IR absorption (top) and Raman scattering (bottom) spectra of $Na_2Ca_2(CO_3)_3$.

spectrum of the lattice region. In the former case, the contributions of atoms are 9 and 85% for Na2 and O2; therefore, this vibration represents rotations of carbonate groups $C1O_3$. The second vibration, where the contribution of $C1O_3$ is 95%, corresponds to rocking of carbonate groups in direction z. The mode of symmetry A_2 with a wave number of 202.3 cm^{-1} has a considerable intensity. Such vibrations are produced by x-displacements of atoms Ca, C1, O1, and O4. Atoms O2 may move in all three directions for all symmetries.

A significantly higher number of vibrations are present in the IR lattice region of carbonate K-Ca (Fig. 4). The most intense ones for symmetry A (E) are the modes with wave numbers of 184.7 and 246.8 cm^{-1} (215.1 and 266.7 cm^{-1}). The polarization vectors of one-fold modes are formed by z-displacements (and, for two-fold modes, xy-displacements) of atoms K1, Ca1 and xyz-displacements of the remaining ones. The first mode of symmetry A is produced by displacements of K1 (8%), Ca2 (18%), and $C1O_3$ (72%), while atoms Ca1, Ca2 (25% each) and $C1O_3$ (49%) contribute to the second one. The lower vibration of symmetry E is formed by displacements of calcium atoms and $C1O_3$ (61%). Vibrations of symmetry E with wave numbers of 173.3, 238.5 cm^{-1} have high intensity in RS spectra. The displacements of atoms O1, O2, O3 produce the dominant (90 and 87%) contribution to their polarization vectors, while calcium atoms play a minor role.

Intramolecular region $\nu 4$ in Na-Ca is formed by five low-intensity vibrations, prominent among which are the modes with wave numbers of 690.7, 718.2, and 731.7 cm^{-1}. The first two are produced almost exclusively by $C1O_3$ ions, while the last one is produced by $C2O_3$. In carbonate K-Ca, there are eight corresponding vibrations with a maximum at a wave number of 703.7 cm^{-1}. The maximum of region ν_2 in the first carbonate and in the second one corresponds to 867.8 cm^{-1} (symmetry A_1, 100% $C1O_3$) and 878.8, 886.4 cm^{-1} (symmetry E). Vibrations type $\nu 1$ are active in both IR and RS. In the former case, their intensity is low; in the latter case, they have the maximum intensity. In carbonate K-Ca, the intensity of the mode of symmetry A with a wave number of 1082.0 cm^{-1} was taken as 100%. Interval $\Delta\nu 1$ in this carbonate is just 1.6 cm^{-1} in magnitude, while the same interval in Na-Ca is 16.9 cm^{-1}. Vibration type $\nu 3$ of symmetry E with a wave number of 1436.7 cm^{-1} is the most intense (6802 km/mol, taken as 100%) in IR K-Ca. This is a vibration with a wave number of 1403.8 cm^{-1} for light polarization along axis z. The displacements of anion $C1O_3$ atoms produce a 34, 100, and 100% contribution to the most intense vibrations with wave numbers of 1495.7, 1477.8, and 1432.3 cm^{-1} in Na-Ca, respectively.

The calculated RS spectra are in a satisfactory agreement with the experimental spectra measured in ambient conditions for $Na_2Ca(CO_3)_3$ in [5,19,21,22]. In the lattice

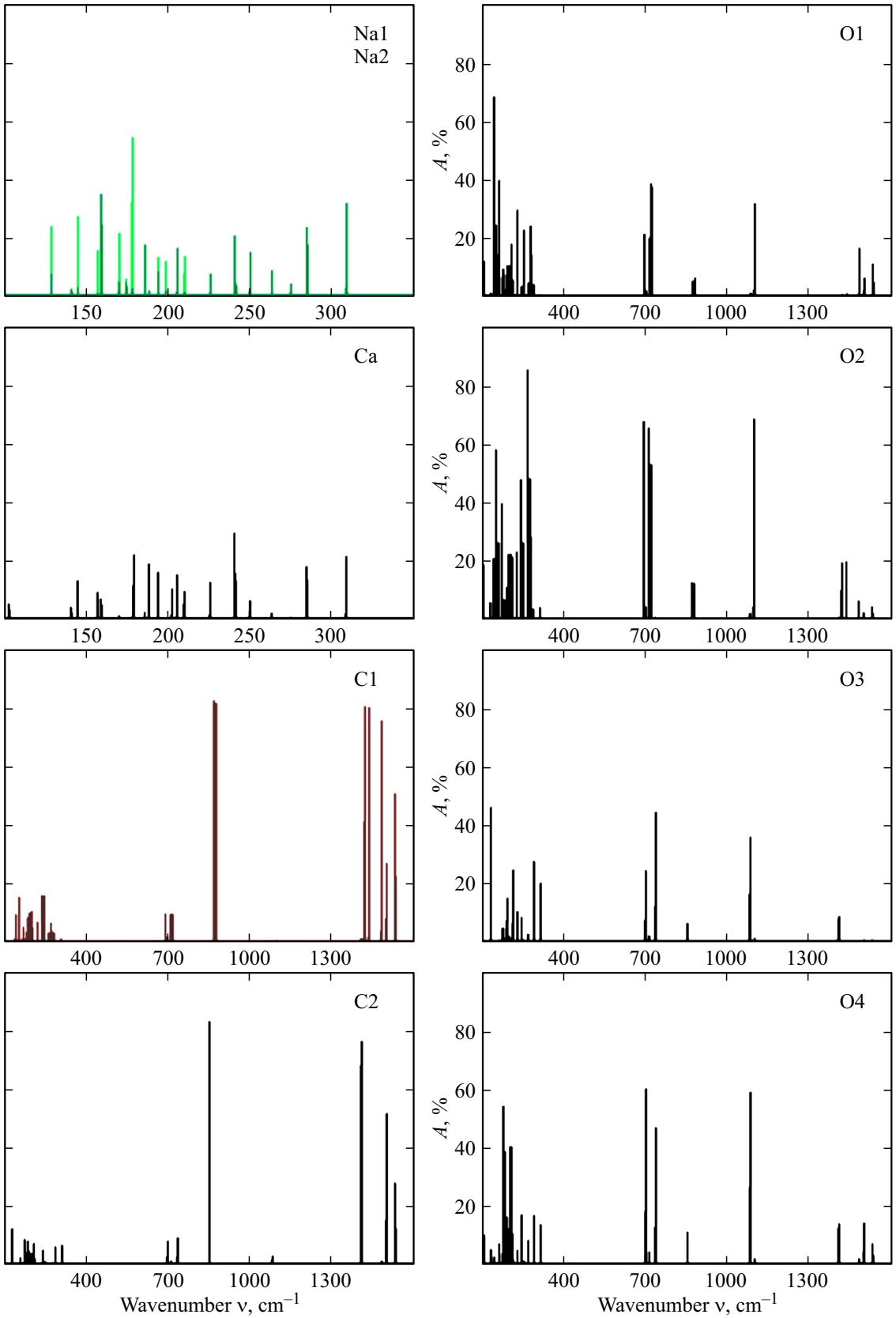

Figure 3. Relative amplitudes A of displacements of non-equivalent atoms in a lattice cell for vibrations with wave numbers ν.

Table 3. Wave numbers ν_i (cm^{-1}) and Grüneisen mode parameters γ_i (in brackets) for normal long-wave vibrations of double carbonates $A_2Ca_2(CO_3)_3$

ν_i (γ_i) $Na_2Ca_2(CO_3)_3$				ν_i (γ_i) $K_2Ca_2(CO_3)_3$	
A_1(IR, RS)	A_2(RS)	B_1(IR, RS)	B_2(IR, RS)	A(IR, RS)	E(IR, RS)
144.6(2.47)	102.7(3.10)	140.8(0.32)	128.4(2.07)	101.6(1.92)	91.9(1.88), 122.8(1.73)
156.7(2.07)	148.5(3.11)	177.9(1.92)	159.0(0.73)	164.3(1.84)	137.5(2.14), 145.8(1.82)
185.6(1.08)	178.9(0.57)	188.3(2.06)	169.9(1.42)	184.7(1.75)	162.9(2.14), 173.3(1.90)
193.8(3.08)	202.3(1.55)	198.4(3.03)	174.2(1.20)	193.7(1.60)	186.7(1.76), 198.0(1.78)
205.4(1.39)	265.3(1.07)	241.2(2.22)	209.8(0.89)	202.8(1.61)	215.1(1.74), 226.8(1.27)
240.6(2.73)		250.0(2.11)	225.7(2.14)	230.5(1.60)	238.5(1.34), 248.9(1.57)
274.8(1.12)		284.8(2.19)	263.3(1.53)	281.0(1.22)	266.7(1.20), 271.7(1.17)
		308.9(0.39)		291.5(1.29)	288.4(1.30)
695.1(0.26)	715.0(0.15)	690.7(0.28)	718.3(0.17)	706.0(0.18)	695.4(0.20), 703.7(0.21)
709.2(0.31)		731.7(0.39)		713.1(0.10)	708.1(0.10), 712.2(0.14)
867.8(−0.01)		875.3(0.03)	848.8(−0.02)	885.1(0.04)	878.8(0.01), 886.4(0.06)
1078.5(0.31)		1094.2(0.29)		1080.9(0.18)	1080.4(0.18),
1095.4(0.27)				1082.0(0.18)	1081.8(0.18)
1403.9(0.27)	1416.4(0.32)	1495.7(0.18)	1432.3(033)	1403.8(0.15)	1397.3(0.21)
1477.8(0.23)		1527.9(0.24)		1447.2(0.25)	1436.7(0.25)
				1474.9(0.23)	1461.8(0.19)
				1491.9(0.19)	1491.6(0.17)

region, features at wave numbers of 133, 140, 171, 199, and 269 cm^{-1} [5] or 132, 139, 171, 203, and 262 cm^{-1} [19] have been identified. Intense modes of symmetry B_2 (128.4, 174, 264.3 cm^{-1}), B_1 (140.8 cm^{-1}), A_1 (144.6, 198.4 cm^{-1}), and A_2 (202.3, 265.3 cm^{-1}) correspond to them in Table 3. The theoretical values of modes of symmetry A_1 and B_1 for intramolecular vibrations $\nu 1$ are 4–6 cm^{-1} above the experimental interval of 1069–1072 cm^{-1} and 1089–1091 cm^{-1}. The same difference is found for modes $\nu 3$, which have been examined experimentally in [52]. The $\nu 3$ frequencies have been measured in IR absorption spectra in [21]: 1387, 1403 1436, 1466, and 1535 cm^{-1}. The values of 694, 710, 718, and 730 cm^{-1}, which agree with the data from [7,52], have been determined for $\nu 4$ in [21]. The wave numbers listed in the table are in a satisfactory agreement with these results, validating the theoretical model.

The RS spectra of $K_2Ca_2(CO_3)_3$ at 773 K have been measured in [14]. An intense peak at 167 cm^{-1}, moderate-intensity peaks at 101 and 221 cm^{-1}, a shoulder at 234 cm^{-1}, and a weak peak at 125 cm^{-1} have been identified in the lattice region. The wave numbers determined with the intensity taken into account (see Table 3) are higher than the experimental ones. This may be attributed to temperature effects, since the temperature in calculations was set to 0 K by default. The values of 705, 711 cm^{-1} and 1076, 1078 cm^{-1} have been established for intramolecular vibrations $\nu 4$ and $\nu 1$ in [14]. The spectral maxima in Fig. 2 are very close to these wave numbers. The same is true for the low-intensity region of asymmetric stretching vibrations $\nu 3$ (CO_3^{2-}) within the 1402–1487 cm^{-1} interval [14] (and the calculated 1397.3–1491.9 cm^{-1} range).

The calculated electron components of static dielectric constant tensor ε_{ij}^{el} are $\varepsilon_{xx} = 2.264$, $\varepsilon_{yy} = 2.257$, and $\varepsilon_{zz} = 2.175$ in carbonate Na-Ca and $\varepsilon_{xx} = \varepsilon_{yy} = 2.234$ and $\varepsilon_{zz} = 2.275$ in K-Ca. The ionic component of the dielectric constant is determined by estimating phonon modes

$$\varepsilon_{ij} = \varepsilon_{ij}^{el} + \frac{4\pi}{V}\Sigma_n \frac{Z_{n,i}Z_{n,j}}{\nu_n^2},$$

where summation is carried out over phonon modes and $Z_{n,i}$ is the effective Born vector that is defined via the Born dynamic charge tensor. The combined components of the dielectric constant tensor for both carbonates are 8.027, 5.910, 7.230 and 7.635, 6.941, respectively. When the coherent displacement of crystal nuclei is factored in, an additional contribution, which depends on the dynamic dielectric constant tensor and the effective Born charge tensor and induces LO-TO splitting, emerges. Figure 5

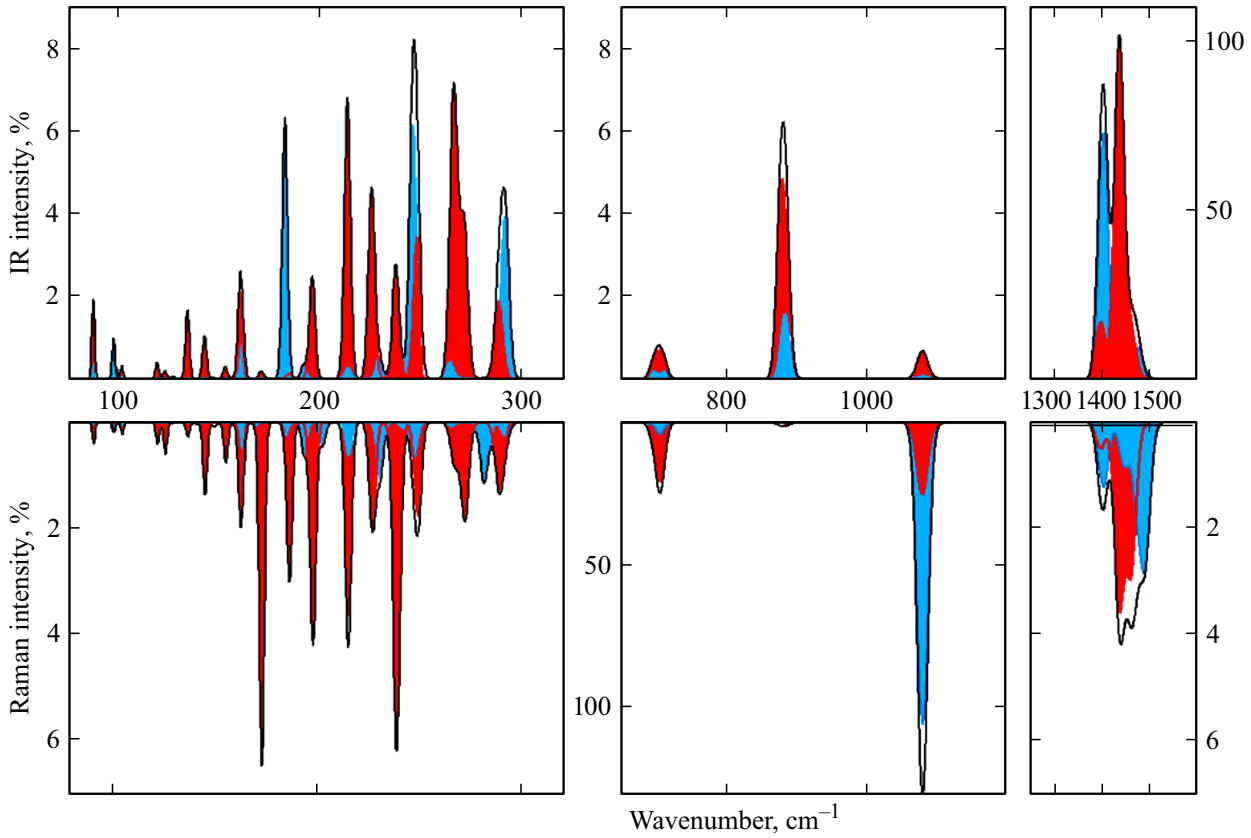

Figure 4. IR absorption (top) and RS (bottom) spectra of $K_2Ca_2(CO_3)_3$.

presents the polarized real parts of the complex reflectance of carbonates. The maxima and minima of spectra correspond to TO and LO frequencies, and the width of each band characterizes LO-TO splitting $\Delta\nu$. The wave numbers of the majority of LO vibrational modes are higher than those of TO modes. Specifically, the values of $\Delta\nu$ for the most intense lattice vibrations of symmetry in carbonate Na-Ca are 146.8, 134.3, and 89.2 cm^{-1}. The wave numbers of LO modes for intramolecular vibrations of symmetry A_1 are $\nu 2 = 875.7\,\text{cm}^{-1}$ and $\nu 3 = 1424.6$, 1530.6 cm^{-1}. The wave numbers of modes $\nu 3$ for symmetry B_2 and B_1 are even higher (1537.0 and 1601.7 cm^{-1}). At the same time, splitting $\Delta\nu$ is negative for certain lattice modes. For example, the values of $\Delta\nu$ for the low-intensity LO mode with wave numbers of 232.1 (A_1), 255.3 (B_2), and 304.1 (B_1) are -7.6, -6.7, and $-4.2\,\text{cm}^{-1}$. The magnitude of splitting for modes $\nu 4$, $\nu 1$ is on the order of 1 cm^{-1}.

The most intense LO modes of symmetry A in carbonate K-Ca are 346.9 cm^{-1} ($\Delta\nu = 57.7\,\text{cm}^{-1}$) and 1524.7 cm^{-1} (119.0 cm^{-1}), while the corresponding modes for symmetry E are 346.0 (54.7), 880.4 (2.5), 890.4 (2.8), 1402.6 (3.6), and 1526.8 (89.5) cm^{-1}. This compound is distinguished by negative splittings corresponding to asymmetric stretching vibrations type $\nu 3$.

Effect of pressure on vibrational spectra

The shortening of interatomic distances under pressure is accompanied by an increase in frequencies of vibrational modes. Therefore, the energy of zero-point vibrations

$$E_0 = \Sigma_{i=1}^{N} \frac{h\nu_i}{2}$$

increases with pressure P. In Na-Ca, this may be characterized by quadratic dependence

$$E_0(\text{kJ/mol}) = 145.39 + 1.33P - 0.03P^2,$$

while K-Ca has

$$E_0(\text{kJ/mol}) = 286.61 + 2.77P - 0.07P^2.$$

Figure 6 presents the dependences of wave numbers of lattice vibrations of carbonate Na-Ca on pressure P and the IR absorption spectrum calculated at 6 GPa. Other double carbonates have similar dependences [53]. The $\nu(P)$ dependence for the most intense lattice vibration of symmetry A_1 is near-linear in nature. Derivative $d\nu/dP$ indicates the rate at which the wave number increases with pressure. In the present case, it is equal to 9.32 cm^{-1}/GPa. Multiplying it by bulk modulus B_0 from Table 2 and dividing by $\nu_0 = 193.8\,\text{cm}^{-1}$, one determines the value of

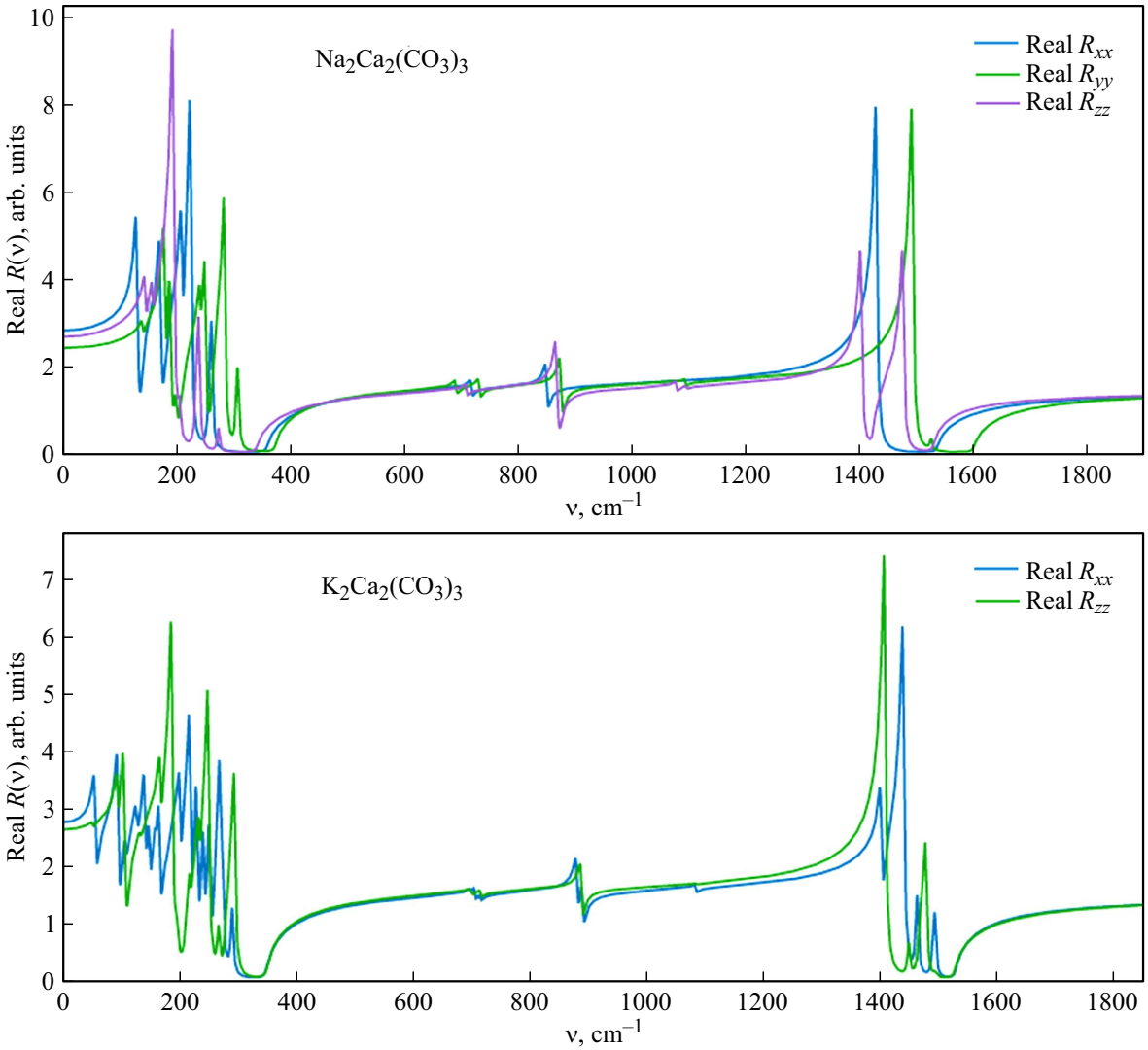

Figure 5. Real part of the complex reflectance of $Na_2Ca_2(CO_3)_3$ (top) and $K_2Ca_2(CO_3)_3$ (bottom). Different colors correspond to xx-, yy-, and zz-components.

the Grüneisen mode parameter: 3.08. The values of γ_i for all wave numbers are listed in Table 3. Second derivative $d^2\nu/dP^2$ characterizes the degree of nonlinearity, and it is equal to $-0.63\,\text{cm}^{-1}/\text{GPa}^2$ for this mode. This is a fairly high value; for example, the first and second derivatives for the mode of symmetry B_2 are $7.53\,\text{cm}^{-1}$/GPa ($\gamma = 2.14$) and $-0.14\,\text{cm}^{-1}/\text{GPa}^2$, respectively.

The dependence of vibrational frequencies for shortite on pressure has been examined in [5,19]. The pressure derivatives for five lattice modes assume the values of 0.8(1), 1.4(1), 1.8(1), 1.8(1), and $3.4(3)\,\text{cm}^{-1}$/GPa in [19] and 0.71(2), 1.23(5), 1.88(8), 3.48(5), and $5.04(1)\,\text{cm}^{-1}$/GPa in [5]. The discrepancies are attributable, among other factors, to the composition of natural minerals: $Na_{1.9}Ca_{2.1}(CO_3)_3$ [5], $Na_{1.94}Ca_{2.02}Sr_{0.01}K_{0.01}(CO_3)_3$ [19]. An ideal stoichiometric formula was used for calculations. It follows from Table 3 that the theoretical and experimental values are in a satisfactory agreement. Derivative $d\nu/dP$ for $\nu 4$ (CO_3^{2-}) $696\,\text{cm}^{-1}$ was found to be equal to $2.59(3)\,\text{cm}^{-1}$/GPa in [5] (2.5(2) in [19]). The derivative for the mode of symmetry A_1 with a wave number of $695.2\,\text{cm}^{-1}$ active in the RS spectrum (4% intensity) is $2.77\,\text{cm}^{-1}$/GPa, while the corresponding value for the mode with $709.2\,\text{cm}^{-1}$ (3%) is $3.41\,\text{cm}^{-1}$/GPa (1.63(6) [5], 2.4(3) [19]). The discrepancies are more significant here. An overestimated value of the derivative ($4.46\,\text{cm}^{-1}$/GPa; 3.17(9) [5], 3.4(2) [19]) was also obtained for the mode of symmetry B_1 with $\nu = 731.7\,\text{cm}^{-1}$. The pattern is the same for mode $\nu 1$ with wave numbers of 1078.5 and $1095.4\,\text{cm}^{-1}$: the determined values of the derivative are 5.22 and $4.62\,\text{cm}^{-1}$/GPa (3.50(5), 4.12(4) [5]; 4.5(3), 5.2(3) [19]).

The pressure dependence for $\nu 2$ (CO_3^{2-}) differs fundamentally from those of other intramolecular modes. For example, the mode of symmetry A_1 with a wave number of $867.8\,\text{cm}^{-1}$ remains almost unchanged when

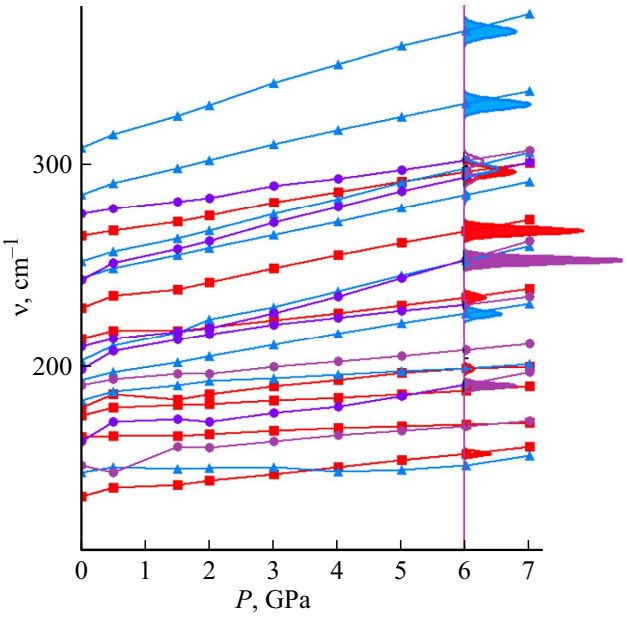

Figure 6. Dependences of wave numbers ν on pressure P for the lattice modes of symmetry A_1 (circles, purple), B_1 (triangles, blue), and B_2 (squares, red) in $Na_2Ca_2(CO_3)_3$. The IR intensities for a pressure of 6 GPa are indicated.

the pressure rises; in fact, it decreases slightly at a rate of $-0.15\,\mathrm{cm}^{-1}$/GPa, while the mode of symmetry B_2 with a wave number of $848.8\,\mathrm{cm}^{-1}$ decreases at a rate of $-0.28\,\mathrm{cm}^{-1}$/GPa. Mode $\nu 2$ behaves in a similar fashion in other carbonates [52].

The RS spectra of K-Ca have been examined in [2,54] under a pressure of 3 GPa and at a high temperature of 1273 K. The authors of [54] have identified the following vibrations in the lattice region: 64, 97, 164, $220\,\mathrm{cm}^{-1}$; for $\nu 4$: 692, 703, $709\,\mathrm{cm}^{-1}$; for $\nu 1$: 1075, $1090\,\mathrm{cm}^{-1}$; and low-intensity vibrations for $\nu 3$: 1400, 1466, 1484, $1515\,\mathrm{cm}^{-1}$. One may use the data from Table 3 and the following formula to obtain calculated values corresponding to this pressure:

$$\nu(P) \approx \nu_0 + \frac{\partial \nu}{\partial P} P.$$

The results of direct calculations at 3 GPa in each region agree fairly well with the experimental data given above: 52.4, 100.1, 170.7, $219\,\mathrm{cm}^{-1}$; 703.8, 712.4, $718.3\,\mathrm{cm}^{-1}$; 1091.6, $1093.3\,\mathrm{cm}^{-1}$; 1414.7, 1467.5, 1494.2, $1506.5\,\mathrm{cm}^{-1}$. Temperature effects should be taken into account when one compares these data sets. Parameters γ_i for lattice modes fall within the interval of 1–2, while the parameters for intramolecular modes are an order of magnitude lower. The wave numbers of vibrations type $\nu 2$ increase with pressure at a rate of just $0.1\,\mathrm{cm}^{-1}$/GPa (for symmetry A) and 0.4, $0.8\,\mathrm{cm}^{-1}$/GPa (for symmetry E).

The established dependences may be used to solve an inverse problem: determine pressure P when wave number ν is known. Specifically, the corresponding formula for the lattice mode of symmetry A_1, which is the most intense in Na-Ca, is

$$P(\mathrm{GPa}) = 105.06 - 1.165\nu + 0.003\nu^2,$$

where ν is expressed in cm^{-1}. For example, $P = 2.06$ GPa is found for $\nu = 212\,\mathrm{cm}^{-1}$ (rigorous calculations yield a value of 2.0 GPa). A linear pressure dependence is obtained for mode $\nu 1$ with a wave number of $1078.5\,\mathrm{cm}^{-1}$:

$$P(\mathrm{GPa}) = -249.9 + 2.232\nu.$$

A similar formula from [19] is written as

$$P(\mathrm{GPa}) = -207.59 + 0.1902\nu(\mathrm{cm}^{-1})$$

with an accuracy of 0.2 GPa. The corresponding linear dependence for vibration $\nu 3$ of symmetry B_1 , which is the most intense in IR, is

$$P(\mathrm{GPa}) = -387.9 + 0.259\nu,$$

where the error of the pressure value determined for a certain calculated wave number is no worse than 0.2 GPa. The formula for a similar vibration of symmetry E in K-Ca is

$$P(\mathrm{GPa}) = -242.4 + 0.169\nu.$$

The vibration of symmetry A, which is the most intense in RS spectra, has

$$P(\mathrm{GPa}) = -286.6 + 0.265\nu.$$

Conclusion

Three vibrations of different polarizations with wave numbers of 193.8, 225.7 and $284.8\,\mathrm{cm}^{-1}$ are the most intense in the lattice region of IR absorption spectra of carbonate Na-Ca, while the modes with wave numbers of 184.7, $246.8\,\mathrm{cm}^{-1}$ and 215.05, $266.7\,\mathrm{cm}^{-1}$ are the most intense for z and xy polarizations, respectively, in carbonate K-Ca. The modes of symmetry B_2, A_1 with wave numbers of 263.3 and $274.8\,\mathrm{cm}^{-1}$ stand out in the RS spectrum of Na-Ca, and the modes of symmetry E with wave numbers of 173.3, $238.5\,\mathrm{cm}^{-1}$ are prominent in the K-Ca spectrum. These vibrations correspond to the rotational motion of carbonate ions. The spectra of these two compounds in the region of intramolecular CO_3^{2-} vibrations are qualitatively similar. The band formed by the type $\nu 3$ mode of symmetry B_1 with a wave number of $\sim 1496\,\mathrm{cm}^{-1}$ (Na-Ca) and $1437\,\mathrm{cm}^{-1}$ (K-Ca) is dominant in IR. Mode $\nu 1$ of symmetry A_1 with a wave number of $\sim$ 1095 and 1082 cm^{-1} has the highest intensity in RS. Higher wave numbers in Na-Ca correspond to shorter interatomic distances in this carbonate.

Different types of lattice and intramolecular vibrations have different rates of growth of wave numbers with pressure. The typical Grüneisen mode parameter for intramolecular vibrations type $\nu 4$ (in-plane deformations),

$\nu 1$ (symmetric in-plane stretching), and $\nu 3$ (asymmetric in-plane stretching) is 0.2−0.4. The parameters for out-of-plane deformations $\nu 2$ are negative in Na-Ca and positive (near-zero) in K-Ca. The established linear relations between wave numbers and pressure may be used to estimate pressures based on known wave number values (and vice versa).

References

[1] Y. Song, M. Luo, D. Zhao, G. Peng, C. Lin, N. Ye. J. Materials Chemistry C, **5** (34), 8758 (2017). DOI: 10.1039/C7TC02789C

[2] A.V. Arefiev, A. Shatskiy, I.V. Podborodnikov, S.V. Rashchenko, A.D. Chanyshev, K.D. Litasov. Phys. and Chem. Minerals, **46**, 229 (2019). DOI: 10.1007/s00269-018-1000-z

[3] I.V. Podborodnikov, A. Shatskiy, A.V. Arefiev, S.V. Rashchenko, A.D. Chanyshev, K.D. Litasov. Phys. and Chem. Minerals, **45**, 773 (2018). DOI: 10.1007/s00269-018-0961-2

[4] Y. Liu, Y. Shen, S. Zhao, J. Luo. Coord. Chem. Rev., **407**, 213152 (2020). DOI: 10.1016/j.ccr.2019.213152

[5] C.E. Vennari, C.M. Beavers, Q. Williams. J. Geophys. Research: Solid Earth, **123** (8), 6574 (2018). DOI: 10.1029/2018JB015846

[6] A.V. Golovin, I.S. Sharygin, A.V. Korsakov, V.S. Kamenetsky, A. Abersteiner. J. Raman Spectrosc., **51** (9), 1849 (2020). DOI: 10.1002/jrs.5701

[7] M. Fastelli, A. Zucchini, P. Comodi, A. Maturilli, G. Alemanno, E. Palomba, R. Piergallini. Minerals, **11**, 845 (2021). DOI: 10.3390/min11080845

[8] W.V. Boynton, D.W. Ming, S.P. Kounaves, S.M.M. Young, R.E. Arvidson, M.H. Hecht, J. Hoffman, P.B. Niles, D.K. Hamara, R.C. Quinn, P.H. Smith, D.C. Catling, R.V. Morris. Science, **325**, 61 (2009). DOI: 10.1126/science.1172768

[9] A.V. Golovin, I.S. Sharygin, A.V. Korsakov. Chem. Geology, **455** (20), 357 (2017). DOI: 10.1016/j.chemgeo.2016.10.036

[10] A.J. Elliot, D.M. Jenkins, T.K. Lowenstein, A.R. Carroll. Geochim. Cosmochim. Acta, **115** (15), 31 (2013). DOI: 10.1016/j.gca.2013.04.005

[11] B. Dickens, A. Hyman, W.E. Brown. J. Research of the National Bureau of Standards A: Phys. and Chem., **75A** (2), 129 (1971). DOI: 10.6028/jres.075A.013

[12] D.S. Robertson, N. Shaw, I.M. Young. J. Mater. Sci., **14**, 230 (1979). DOI: 10.1007/BF01028348

[13] A.V. Arefiev, A. Shatskiy, I.V. Podborodnikov, A. Bekhtenova, K.D. Litasov. Minerals, **9** (5), 296 (2019). DOI: 10.3390/min9050296

[14] V. Arefiev, I.V. Podborodnikov, A.F. Shatskiy, K.D. Litasov. Geochem. International, **57** (9), 981 (2019). DOI: 10.1134/S0016702919090039

[15] A. Navrotsky, R.L. Putnam, C. Winbo, E. Rose'n. American Mineralogist, **82** (5−6), 546 (1997). DOI: 10.2138/am-1997-5-614

[16] C. Winbo, E. Rosen, M. Heim. Acta Chem. Scand., **52**, 431 (1998). DOI: 10.3891/acta.chem.scand.52-0431

[17] C. Winbo, D. Bostroem, M. Goebbels. Acta Chem. Scand., **51** (3), 387 (1997). DOI: 10.3891/ACTA.CHEM.SCAND.51-0387

[18] I.V. Podborodnikov, A. Shatskiy, A.V. Arefiev, K.D. Litasov. Lithos, **330**−**331**, 74 (2019). DOI: 10.1016/j.lithos.2019.01.035

[19] U. Borodina, A. Likhacheva, A. Golovin, S. Goryainov, S. Rashchenko, A. Korsakov. High Pressure Research, **38** (3), 293 (2018). DOI: 10.1080/08957959.2018.1488973

[20] Q.C. Williams, C. Vennari, E.F. III O'Bannon. Am. Geophys. Union, Fall Meeting abstract id. MR13B-2703 (2015).

[21] L. Ray, F. Marilla, J. Dickfos. Spectrochim. Acta, Part A: Molec. and Biomolec. Spectrosc., **71** (1), 143 (2008). DOI: 10.1016/j.saa.2007.11.021

[22] S.V. Goryainov, S.N. Krylova, U.O. Borodina, A.S. Krylov. J. Phys. Chem. C, **125** (33), 18501 (2021). DOI: 10.1021/acs.jpcc.1c05077

[23] T. Inerbaev, P. Gavryushkin, K. Litasov, F. Abuova, A. Akilbekov. Bulletin of the Karaganda University: Phys. Ser., **4** (88), 24 (2017). DOI: 10.31489/2017Phys4/24-34

[24] R. Dovesi, A. Erba, R. Orlando, C.M. Zicovich-Wilson, B. Civalleri, L. Maschio, M. Rérat, S. Casassa, J. Baima, S. Salustro, B. Kirtman. WIREs Comput. Mol. Sci., **8** (4), e1360 (2018). DOI: 10.1002/wcms.1360

[25] A.D. Becke. J. Chem. Phys., **98**, 5648 (1993). DOI: 10.1063/1.464913

[26] C. Lee, W. Yang, R.G. Parr. Phys. Rev. B, **37**, 785 (1988). DOI: 10.1103/PhysRevB.37.785

[27] L. Valenzano, F.J. Torres, K. Doll, F. Pascale, C.M. Zicovich-Wilson, R. Dovesi. Z. Phys. Chem., **220**, 893 (2006). DOI: 10.1524/zpch.2006.220.7.893

[28] R. Dovesi, C. Roetti, C. Freyria Fava, M. Prencipe, V.R. Saunders. Chem. Phys., **156** (1), 11 (1991). DOI: 10.1016/0301-0104(91)87032-Q

[29] R. Dovesi, V. R. Saunders, C. Roetti, R. Orlando, C.M. Zicovich-Wilson, F. Pascale, B. Civalleri, K. Doll, N. M. Harrison, I.J. Bush, P. D'Arco, M. Llunel, M. Causa, Y. Noel, L. Maschio, A. Erba, M. Rerat, S. Casassa. CRYSTAL17 user'smanual (2018). URL: https://www.crystal.unito.it/index.html

[30] H.J. Monkhorst, J.D. Pack. Phys. Rev. B, **13**, 5188 (1976). DOI: 10.1103/PhysRevB.13.5188

[31] F. Pascale, C.M. Zicovich-Wilson, F. Lopez, B. Civalleri, R. Orlando, R. Dovesi. J. Comput. Chem., **25**, 888 (2004). DOI: 10.1002/jcc.20019

[32] C.M. Zicovich-Wilson, F. Pascale, C. Roetti, V.R. Saunders, R. Orlando, R. Dovesi. J. Comput. Chem., **25**, 1873 (2004). DOI: 10.1002/jcc.20120

[33] L. Maschio, B. Kirtman, M. Rerat, R. Orlando, R. Dovesi. J. Chem. Phys., **139**, 164101 (2013). DOI: 10.1063/1.4824442

[34] M. Ferrero, M. Rérat, R. Orlando, R. Dovesi. J. Comp. Chem., **29** (9), 1450 (2008). DOI: 10.1002/jcc.20905

[35] M. Ferrero, M. Rérat, R. Orlando, R. Dovesi. J. Chem. Phys., **128**, 014110 (2008). DOI: 10.1063/1.2817596

[36] M. Ferrero, M. Rerat, R. Orlando, R. Dovesi, I.J. Bush. J. Phys.: Conf. Ser., **117**, 12016 (2008). DOI: 10.1088/1742-6596/117/1/012016

[37] R. Orlando, V. Lacivita, R. Bast, K. Ruud. J. Chem. Phys., **132**, 244106 (2010). DOI: 10.1063/1.3447387

[38] M. Ferrero, M. Rérat, B. Kirtman, R. Dovesi. J. Chem. Phys., **129** (24), 244110 (2008). DOI: 10.1063/1.3043366

[39] M. Ferrero, B. Civalleri, M. Rérat, R. Orlando, R. Dovesi. J. Chem. Phys., **131** (21), 214704 (2009). DOI: 10.1063/1.3267861

[40] R.A. Kumar. J. Chem., **2013**, 154862 (2013). DOI: 10.1155/2013/154862
[41] C. Carteret, M. De La Pierre, M. Dossot, F. Pascale, A. Erba, R. Dovesi. J. Chem. Phys., **138**, 014201 (2013). DOI: 10.1063/1.4772960
[42] A. Grzechnik, P. Simon, P. Gillet, P. McMillan. Physica B: Condens Matter, **262** (1–2), 67 (1999). DOI: 10.1016/S0921-4526(98)00437-2
[43] F. Birch. J. Geophys. Research, **83** (B3), 1257 (1978). DOI: 10.1029/JB083iB03p01257
[44] C. Wu, G. Yang, M.G. Humphrey, C. Zhang. Coord. Chem. Rev., **375** (15), 459 (2018). DOI: 10.1016/j.ccr.2018.02.017
[45] X. Liu, P. Gong, Y. Yang, G. Song, Z. Lin. Coord. Chem. Rev., **400**, 213045 (2019). DOI: 10.1016/j.ccr.2019.213045
[46] Y. Liu, Y. Shen, S. Zhao, J. Luo. Coord. Chem. Rev., **407**, 213152 (2020). DOI: 10.1016/j.ccr.2019.213152
[47] Q. Jing, G. Yang, J. Hou, M. Sun, H. Cao. J. Solid State Chem., **244**, 69 (2016). DOI: 10.1016/j.jssc.2016.08.036
[48] R. Li. Crystals, **7** (2), 50 (2017). DOI: 10.3390/cryst7020050
[49] S.K. Kurtz, T.T. Perry. J. Appl. Phys., **39** (8), 3798 (1968). DOI: 10.1063/1.1656857
[50] Yu.N. Zhuravlev, V.V. Atuchin. Nanomaterials, **10** (11), 2275 (2020). DOI: 10.3390/nano10112275
[51] Y.N. Zhuravlev, V.V. Atuchin. Sensors, **21**, 3644 (2021). DOI: 10.3390/s21113644
[52] H.H. Adler, P.F. Kerr. Am. Mineralogist, **48**, 839 (1963).
[53] Y.N. Zhuravlev. Geochem. International, **60** (11), 1103 (2022). DOI: 10.1134/S0016702922110118
[54] A. Arefiev, A. Shatskiy, A. Bekhtenova, K. Litasov. J. Raman Spectrosc., **53** (12), 2110 (2022). DOI: 10.1002/jrs.6438

Translated by D.Safin